JOURNAL OF MATERIALS SCIENCE 2 (1967) 241–255

The Effect of Particle Content and Matrix Grain Size on the Recrystallisation of Two-Phase Aluminium-Iron Alloys

P. R. MOULD*, P. COTTERILL
Department of Metallurgy and Materials Technology, University of Surrey, London, SW11, UK

Received 4 January 1967

The recrystallisation of aluminium alloys in the composition range 0.002 to 1.08 wt % iron has been followed metallographically and by hardness measurements. The recrystallisation of solid-solution alloys was retarded as the iron content increased, whereas that of the two-phase alloys was accelerated. This latter effect was associated with a marked increase in nucleation rate, with no significant change of growth rate, as the Al_3Fe particle spacing decreased from 15 to 4 μm. Decreasing the grain size of the two-phase alloys, at constant composition, also caused an acceleration of recrystallisation, the magnitude of which decreased as the Al_3Fe content increased. These effects have been shown to be independent of the size of the Al_3Fe particles, within the range studied (diameters 0.6 to 2.2 μm). The results are discussed in terms of a model (which is based on metallographic observations) of nucleation at matrix grain boundaries and at particle/matrix interfaces. It is suggested that the retardation of nucleation, observed by other workers, in more closely spaced dispersions, occurs because nucleation at particle/matrix interfaces becomes difficult when the inter-particle spacing becomes of the same order as the diameter of the sub-structure of the deformed matrix.

1. Introduction

After cold-working, approximately 10% of the energy expended in deformation is stored in a metal [1, 2]. Hence, a cold-worked metal is thermodynamically unstable, and, on annealing, it will revert to a more stable, lower energy state by the thermally activated nucleation, and by growth of new, strain-free grains. The initial grain-size of a deformed metal influences the recrystallisation process in two ways. Firstly, the stored energy of cold-work increases as the grain size decreases [3, 4], as does the dislocation density [5, 6]. Secondly, it has been shown that deformed grain-boundaries can act as nucleation sites [7-10]. Hence, decreasing the grain size of a metal leads, firstly, to a reduction of the recrystallisation temperature [11], since less thermal energy is required to activate the process, and, secondly, to an increase in the number of nuclei, with a consequent reduction in the final grain-size.

It is generally agreed that increasing the solute content of any solid-solution alloy raises the recrystallisation temperature and decreases the rate of recrystallisation, by reducing the mobility of the high-angle boundary which surrounds an expanding new grain [12-14]. However, the effect of dispersed second-phase particles on recrystallisation is considerably less clear, since two different effects have been reported. Some investigators report that recrystallisation is accelerated by the presence of a dispersed second phase [15-19], whereas others report the opposite effect [20-27]. A close examination of the various results suggests that the inter-particle spacing is the controlling factor, acceleration occurring at wide spacings and retardation at close spacings.

Doherty and Martin [28, 29] investigated the behaviour of aluminium-copper alloys with inter-particle spacings in the range 1 to 4 μm. They showed that an alloy having a mean inter-

*Now in the Department of Materials Science and Engineering at Cornell University, New York.

particle spacing of 4 μm recrystallised at a rate which was approximately 100 times faster than that of a solid-solution alloy having the same composition as the dispersion matrix. However, decreasing the spacing to approximately 1.5 μm retarded recrystallisation by approximately 10 times, and a further reduction of the spacing to 1.2 μm retarded the recrystallisation process by a further 1000 times. They also report decreases of a similar magnitude in the nucleation rate, as a function of inter-particle spacing. They point out that viable recrystallisation nuclei have been observed to have a diameter of the order of 1 μm [30], and they interpret their results by proposing that, unless boundaries of nuclei have become mobile before impinging on dispersed particles, nucleation will be difficult and the recrystallisation process will be retarded.

Unfortunately, there have been no quantitative reports of the separate effect of grain size in two-phase alloys. Furthermore, Doherty and Martin were unable to investigate the effect of particle spacings greater than 4 μm, where accelerated recrystallisation can be expected to occur. It was in an attempt to clarify these two aspects of the behaviour of two-phase alloys that the present work was undertaken. The aluminium-iron alloy system was chosen for study, since a wide range of dispersions can be produced by the preliminary hot-working of alloys containing different proportions of the Al-Al_3Fe eutectic. The particles so produced are then incoherent and extremely stable, with little change in solubility at temperatures below 500° C. Hence, recrystallisation experiments can be carried out under a wide variety of conditions at temperatures in the range 200 to 350° C, with no significant change in either the matrix solute content or the particle dispersion parameters.

2. Experimental Techniques

2.1. Alloy Preparation

Of the twelve alloys investigated, three were solid solutions (containing 0.0025, 0.0035, and 0.0045 wt % iron), and nine were two-phase dispersions (compositions in the range 0.008 to 1.08 wt % iron). They were each made by chill-casting appropriate proportions of super-purity aluminium (nominally 99.99%) and a binary master-alloy containing 9.5 wt % iron, care being taken to make further use of those portions of the ingots which had been shown to be free of segregation. Two of the alloys (0.24 and 1.08 wt % iron) were analysed volumetrically: these were then used as standards for the spectrographic analysis of the remaining ten alloys.

The as-cast two-phase alloys were hot-forged in order to produce a uniform dispersion of near-spherical Al_3Fe particles in an aluminium-based solid-solution matrix. All the alloys (i.e. the homogeneous as-cast solid-solutions and the dispersed two-phase alloys) were then given a 30% reduction in thickness by cold-rolling, and annealed for 48 h at 450° C. This treatment had two consequences. Firstly, it produced a fully recrystallised structure, with an acceptable degree of grain refinement, in all the alloys. Secondly, it ensured that the solute content of the matrix in each of the two-phase dispersions was equal to the equilibrium solubility limit at 450° C (see appendices, section A.2). Additional samples of the two-phase alloys containing 0.008 wt % iron and 0.86 wt % iron were subjected to a variety of deformations prior to being annealed for 48 h at 450° C in order to produce a range of matrix grain sizes at each of these compositions.

2.2. Measurement of Grain Size and Particle Dispersion Parameters

Metallographic specimens were prepared by electropolishing in a perchloric acid solution followed by etching in a mixed aqueous solution of hydrofluoric, hydrochloric, and nitric acids. The grain size was measured by a lineal count method using the number of grain boundaries crossed in a known distance to calculate the average grain-diameter. The particle radius (r) and the inter-particle spacing ($2R$) were calculated by means of the formula developed by Shaw *et al* [31] and used by Doherty and Martin [28, 29]. The number of particles present was calculated by counting particles in ten randomly positioned areas for each of two specimens of each dispersion alloy, the final result being expressed as the number of particles per unit of specimen surface (N_A).

2.3. Recrystallisation Experiments

All samples were given a final deformation of 60% reduction in thickness by cold-rolling at room temperature. Two types of annealing treatment were then used to produce recrystallisation; viz. isochronal annealing for 1 h at temperatures in the range 100 to 400° C, and isothermal annealing at 300° C for times of up

to 1000 min, the accuracy of the temperature measurement being $\pm 1.5°$ C in each case.

The progress of recrystallisation was followed both metallographically and by means of Vickers hardness indentations. Quantitative metallographic assessments were made by means of a lineal count method previously used by Hilliard and Cahn [32], which is based on 100 grid intersections in each of ten randomly selected areas of each specimen. In the case of isochronal annealing, the lowest annealing temperature to produce any observable recrystallised regions was taken as the *recrystallisation start temperature*, and the lowest annealing temperature which produced a completely recrystallised structure was taken as the *recrystallisation finish temperature*. In the case of the isothermally annealed material, a measure of the number of nuclei involved in the recrystallisation process was obtained by counting the number of recrystallised grains in several areas of each specimen. Estimates of the *apparent nucleation rate* ($\dot{N}'$) and the *apparent growth rate* ($\dot{G}'$) were then obtained by the use of the formula of Doherty and Martin [28]: $\dot{N}'$ is the ratio of the number of recrystallised grains per unit volume to the time for completion of recrystallisation; $\dot{G}'$ is the ratio of the average radius of recrystallised grains to the time for completion of recrystallisation. These values are not the same as the conventional values of *nucleation rate* ($\dot{N}$) and *growth rate* ($\dot{G}$), but they are not seriously in error for comparative purposes.

Unfortunately, it was not possible to use the hardness data in order to assess the recrystallisation start temperature, owing to the overlap of softening due to recovery, and to softening due to the early stages of recrystallisation. However, the 50% recrystallisation temperature and the finish recrystallisation temperature were obtained from the hardness data, independently of any recovery softening, by means of the *rate of change* technique, which is described in the appendices (see section A.1).

In all two-phase alloys, experiments were confined to material the average particle diameter of which was within the range 0.5 to 2.5 μm. Since a series of preliminary experiments (which are described in the appendices, section A.2) had shown that the recrystallisation characteristics were independent of the particle size within this range, for a series of three alloys the compositions of which covered the whole of the present series of two-phase alloys.

3. Results

3.1. Grain Size and Dispersion Data

The three solid-solution alloys contained 0.0025, 0.0035, and 0.0045 wt % iron and had grain diameters, immediately prior to cold-rolling and recrystallisation, of 0.38, 0.20, and 0.22 mm, respectively. The grain sizes and dispersion data for the two-phase alloys are listed in table I.

TABLE I Grain-size and dispersion data for the two-phase alloys.

Iron content (wt %)	Grain diameter (mm)	Dispersion data				
		N_A ($\times 10^4$)	r (μm)	R (μm)	$2R$ (μm)	VMFP (μm)
0.008	0.40	4.7	0.30	7.70	15.40	7400
0.013	0.32	7.1	0.33	6.04	12.08	4020
0.04	0.33	18.7	0.42	4.76	9.52	1222
0.06	0.25	35.2	0.38	3.68	7.36	614
0.11	0.20	74.0	0.36	2.86	5.72	257
0.24	0.17	141	0.39	2.36	4.72	168
0.40	0.19	187	0.44	2.23	4.46	111
0.86	0.14	213	0.52	2.05	4.10	60
1.08	0.16	334	0.55	1.98	3.96	50

N_A = number of particles per square centimetre on plane of polish
r = average particle-radius
R = radius of spherical domain for each particle
$2R$ = inter-particle spacing
VMFP = volumetric mean free path

3.2. Isochronal Recrystallisation

The results were plotted as graphs of hardness against annealing temperature. Three typical curves are shown in fig. 1. For all the alloys studied, there was a gradual decrease in hardness (of the order of 30% of the total hardness decrease) which was not accompanied by any

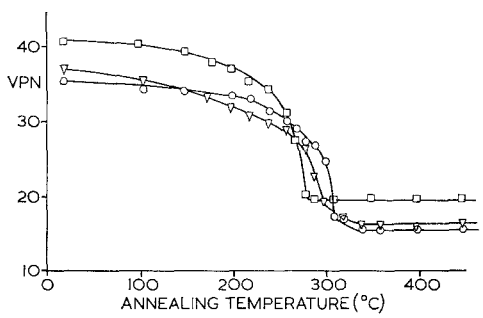

Figure 1 Curves of hardness versus annealing temperature for three two-phase alloys. (O = 0.008 wt % Fe; ▽ = 0.04 wt % Fe; □ = 0.4 wt % Fe.)

observable changes of microstructure, and which was, therefore, attributed to recovery. In each case, the more rapid hardness decrease occurring at higher temperatures coincided with metallographic observations of recrystallisation. Fig. 2 summarises the variation of the temperatures for the start, 50% stage, and finish of recrystallisation as a function of composition, within the range studied (i.e. 0 to 1 wt % iron). There are clearly two separate groups of curves: firstly, the solid-solution alloys (0.0025 to 0.0045 wt % iron), in which there is a marked increase in recrystallisation temperature with increase in iron content; secondly, the two-phase alloys (0.008 to 1.08 wt % iron) for which the reverse was found.

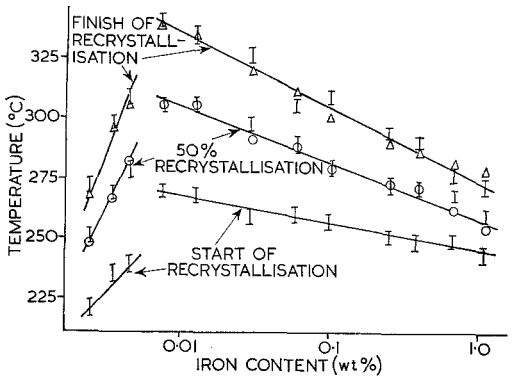

Figure 2 Recrystallisation temperature versus iron content for alloys, the grain-size and dispersion data of which are listed in table I. (I= metallography; O = dH/dT_{max}; △ = dH/dT_{finish}.)

The variation of the recrystallisation temperatures with original grain-size (for invariant composition) is shown in figs. 3 and 4 for alloys containing 0.008 and 0.86 wt % iron respectively. For both alloys, the recrystallisation temperatures increase with increasing grain-size; although a comparison of the two sets of data shows a greater sensitivity for the alloy having lower iron content.

3.3. Isothermal Recrystallisation

Isothermal recrystallisation was studied for three two-phase alloys (0.008, 0.06, and 0.86 wt % iron). Fig. 5 shows typical curves of hardness versus annealing time for samples of these alloys having similar grain-sizes. In all cases (as in the isochronal experiments), there was an initial, gradual hardness decrease which was attributed to recovery, followed by a more rapid softening which coincided with the metallographic observation of recrystallisation. Fig. 6 shows the progress of recrystallisation, as determined by quantitative metallography, as a function of both composition and original grain-size, together with an indication of the time required to produce 50% recrystallisation.

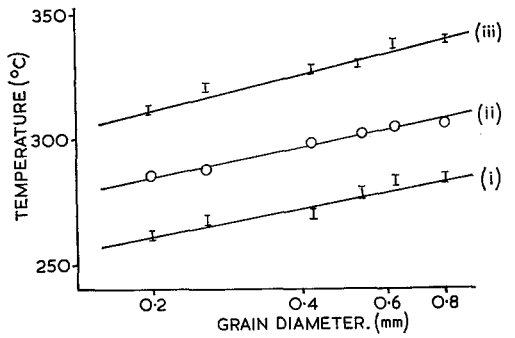

Figure 3 Recrystallisation temperature versus original grain-size for an alloy containing 0.008 wt % iron: (i) start of recrystallisation; (ii) 50% recrystallisation; (iii) finish of recrystallisation (symbols as for fig. 2).

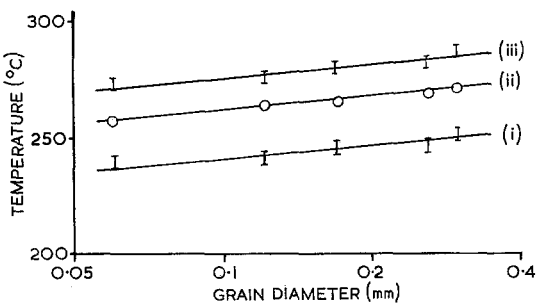

Figure 4 As fig. 3, for an alloy containing 0.86 wt % iron.

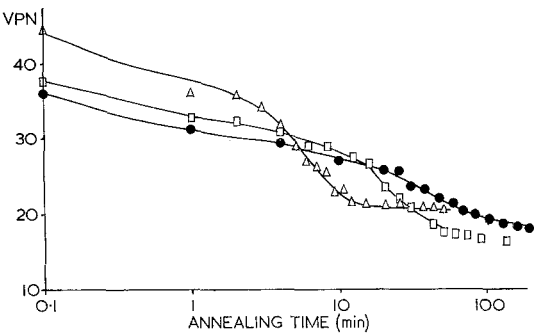

Figure 5 Curves of hardness versus annealing time for three two-phase alloys (● = 0.008 wt % Fe, grain size 0.19 mm; □ = 0.06 wt % Fe, grain size 0.22 mm; △ = 0.86 wt % Fe, grain size 0.16 mm).

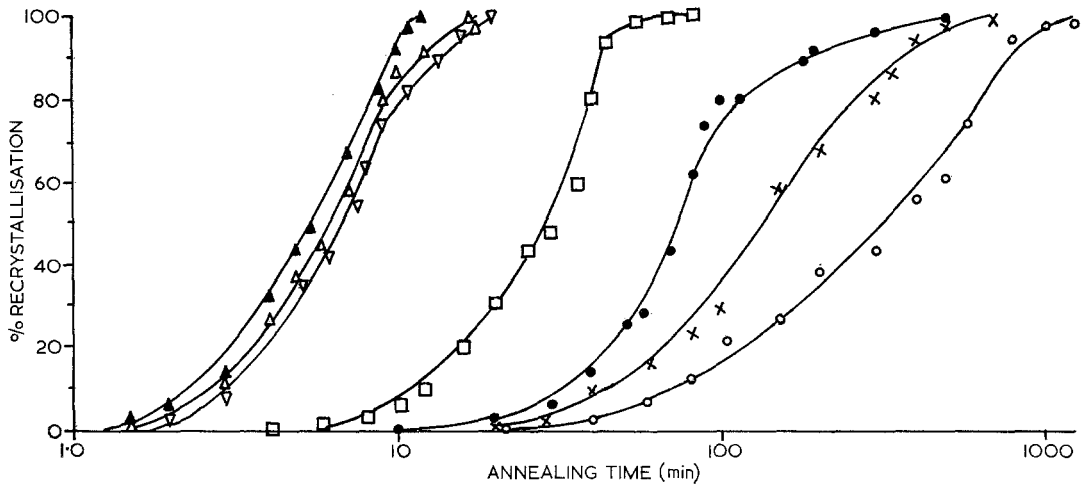

Figure 6 The progress of recrystallisation (determined metallographically) versus annealing time, for various iron contents and grain sizes.

Symbol	▲	△	▽	□	●	×	○
Iron content (wt %)	0.86	0.86	0.86	0.06	0.008	0.008	0.008
Grain diameter (mm)	0.07	0.16	0.30	0.22	0.19	0.37	0.74

Some experimental results are also recorded in table II.

TABLE II Isothermal recrystallisation times (determined metallographically) for three two-phase alloys having similar initial grain-sizes. (See figs. 5 and 6.)

Iron content (wt %)	N_A ($\times 10^4$)	Grain diameter (mm)	Annealing time	
			$t_{50\%}$ (min)	$t_{100\%}$ (min)
0.008	4.7	0.19	78	600
0.06	35.2	0.22	28	80
0.86	213	0.16	6.4	17

$t_{50\%}$ = time to produce 50% recrystallisation
$t_{100\%}$ = time to produce 100% recrystallisation

Unfortunately, the etching characteristics of these alloys were such that conditions which clearly outlined the Al_3Fe particles also led to severe over-etching of the grain boundaries, and vice versa. Hence, photomicrographs have not been reproduced here. However, immediately prior to the final cold-rolling and recrystallisation, it was clear that the particles were, in all cases, homogeneously dispersed throughout the matrix and were not preferentially associated with grain boundaries. Whereas there were clear variations in the location of recrystallisation nucleation sites as a function of composition. In the alloy containing 0.008 wt % iron (i.e. very few particles), recrystallisation was initiated preferentially at the original grain-boundaries; nucleation in the interior regions of original grains was very rare and occurred only in the late stages of the overall recrystallisation process. Conversely, the alloy containing 0.86 wt % iron (with a comparatively high particle density) always had a much more homogeneous distribution of initial recrystallisation sites, some of which were associated with original grain-boundaries, whilst others were clearly situated in the original grain-interiors (possibly at Al_3Fe particles).

Data for the nucleation and growth characteristics of the recrystallised material are shown in figs. 7 and 8. Fig. 7 shows the relationship between the number of nuclei (per unit area of plane section) and the area fraction of recrystallised material as a function of both the iron content and the grain size. Fig. 8 shows the variation of apparent nucleation rate ($\dot{N}'$) and the apparent growth rate (G') with iron content, for similar, initial grain-sizes (i.e. for the conditions represented in fig. 5).

4. Discussion

4.1. Solid-Solution Alloys

The basic objective of the present investigation was to study the effect of second-phase particles on recrystallisation behaviour. Hence, information concerning the recrystallisation of solid-solution alloys is very restricted. However, the

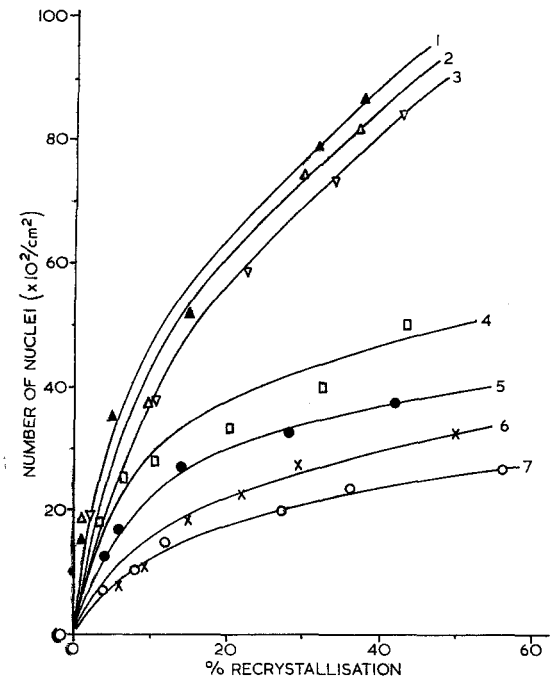

Figure 7 The number of recrystallisation nuclei versus the area fraction of recrystallised material (for various iron contents and grain sizes as given for fig. 6).

Symbol	▲	△	▽	□	●	×	○
Curve number	1	2	3	4	5	6	7

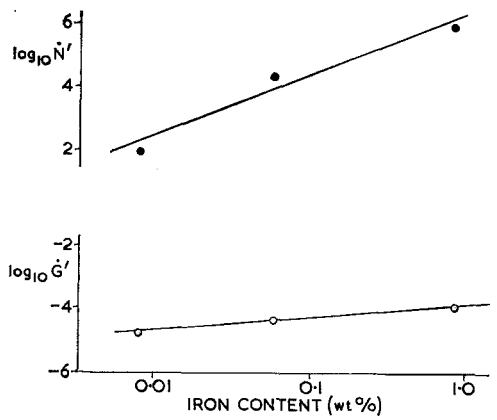

Figure 8 The apparent nucleation rate ($\dot{N}'$) and the apparent growth rate ($\dot{G}'$) versus iron content for three two-phase alloys having similar grain-sizes (see fig. 5 caption).

results summarised in fig. 2 show that increasing the solute content of solid-solution alloys has two separate effects on their isochronal recrystallisation characteristics: firstly, the temperature at which recrystallisation starts is raised; and, secondly, the temperature range required to complete the recrystallisation process (i.e. the difference between the start and finish temperature) is increased.

These observations imply (i) the need for an increasing driving force to initiate recrystallisation, and (ii) a decreasing overall rate of recrystallisation, as the solute content is increased. Each of these conclusions is consistent with previous reports [12-14] that increasing the solute content of a solid solution leads to a decrease in the mobility of high-angle boundaries. However, the present investigations were restricted to isochronal recrystallisation, in the case of solid-solution alloys: consequently, the values of the appropriate nucleation and growth rates remain unknown. Hence, no positive conclusion can be drawn as to the detailed mechanism of this effect.

4.2. Two-Phase Alloys

4.2.1. The Effect of Grain Size on Recrystallisation Temperatures

In the case of two-phase alloys (i.e. iron contents $\geqslant$ 0.008 wt %), fig. 2 shows that as the iron content increases the temperature at which recrystallisation starts decreases, as also does the temperature range required to complete the recrystallisation process. The method of preparation ensured that, in each case, the iron content of the aluminium-rich solid solution was equal to the equilibrium solubility limit at 450° C, whilst separate experiments had shown that their recrystallisation behaviour was independent of particle size (see appendices and table I).

However, reference to table I shows that the original grain-diameter of these alloys decreased as the iron content increased (i.e. from 0.40 mm at 0.008 wt % iron to 0.14 mm at 0.86 wt % iron), whilst figs. 3 and 4 show a clear dependence of recrystallisation temperatures on grain size for both ends of this composition range. Hence, it is necessary to eliminate the separate effect of grain size on recrystallisation behaviour, before attempting to draw conclusions as to the specific effect of second-phase particles. Fig. 3 shows that, for an alloy containing 0.008 wt % iron, the start, 50% stage, and finish recrystallisation temperatures would each be reduced by 17° C as the result of a decrease in grain size from 0.4 to 0.14 mm. Consequently, the recrystallisation temperature lines of fig. 2 can be modified to indicate the true recrystallisation temperatures for alloys of equal original grain-

size (0.14 mm), if the position of the start, 50% stage, and finish recrystallisation temperatures are lowered by 17° C, at 0.008 wt % iron, relative to their position at 0.86 wt % iron. These adjustments are shown in fig. 9, where the broken lines are the experimentally determined lines of fig. 2 and the full lines are the corrected ones indicating the effect of composition for alloys of constant grain-size.

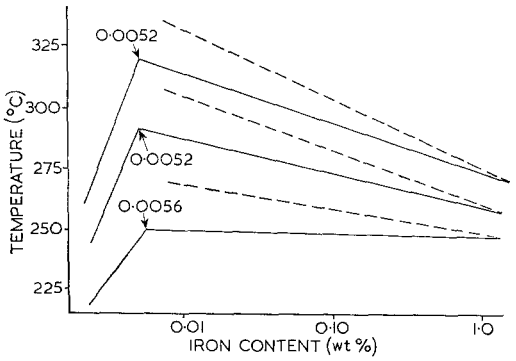

Figure 9 Recrystallisation temperature versus iron content: broken lines represent the experimental results (i.e. alloys of varying grain-size); full lines represent the "correction" to show the effect of composition at constant grain-size (i.e. 0.14 mm).

4.2.2. The Effect of Al_3Fe Particles on Recrystallisation Temperatures

Fig. 9 also shows that the curves of extrapolated recrystallisation temperature versus composition for the two-phase alloys intersect those of the solid-solution alloys at almost identical iron concentrations (average value 0.0053 wt % iron). In view of their preparation history, this should represent the equilibrium solubility of iron in aluminium at 450° C. The nearest known solubility measurement is that of Edgar [33], who determined a solubility of 0.006 wt % iron at 500° C. This is sufficient evidence to conclude that the change in the nature of the recrystallisation characteristics, as a function of composition, occurs as the result of the presence of Al_3Fe particles at iron contents in excess of about 0.005 wt %.

Since the corrected curves shown in fig. 9 represent the recrystallisation temperatures of two-phase alloys (the Al_3Fe particles of which are of approximately constant size, homogeneously distributed within a constant composition aluminium-iron solid-solution of constant grain-size), it is to be expected that the variation of recrystallisation characteristics which they indicate is a function of the number of Al_3Fe particles present in each alloy. This is confirmed by fig. 10, which shows that the relationship

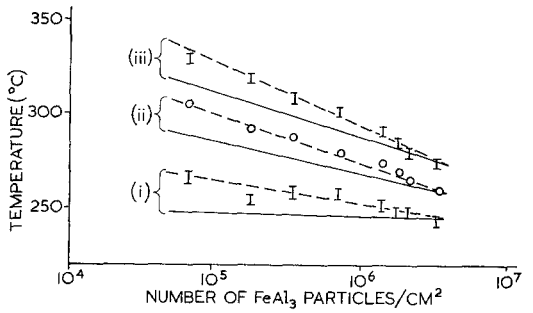

Figure 10 Recrystallisation temperature versus number of second-phase particles (broken and full lines as for fig. 9): (i) start of recrystallisation; (ii) 50% recrystallisation; (iii) finish of recrystallisation (I = metallography; O = dH/dT_{max}).

between the recrystallisation temperatures and the number of Al_3Fe particles is identical in form to that between the recrystallisation temperatures and composition. Whereas plots against other dispersion parameters (volume fraction, inter-particle spacing, etc.) showed much greater scatter. The major effect of the presence of Al_3Fe particles, independently of other microstructural variables, is therefore to decrease the recrystallisation temperature range, from approximately 80° C at 0.008 wt % iron to approximately 30° C at 1.08 wt % iron, in a way which is directly related to the number of particles present, without sensibly altering the temperature at which the recrystallisation process starts.

The results summarised in figs. 9 and 10 also indicate an important aspect of experimental technique, since they are dependent on the criteria which are used to define and determine the recrystallisation temperature. Clearly, if the start of recrystallisation had been taken as the sole criterion for studying the influence of composition, no significant effect would have been reported, whereas if the finish of recrystallisation had been the sole criterion, a large effect would have been reported. It is therefore to be recommended strongly that the full recrystallisation temperature range should always be studied, in order to obtain the most useful information, and to avoid misleading and

unreal inconsistencies concerning the effect of any controlled variables on the recrystallisation process.

4.2.3. Recrystallisation Kinetics

The recrystallisation/time curves in fig. 6 are all of the standard S-curve form, which is characteristically associated with a nucleation and growth process. They show that increasing the iron content (and, therefore, the number of Al_3Fe particles) markedly increases the rate of recrystallisation, for samples of similar, original grain-sizes (see table II for details). This is consistent with the results of the isochronal experiments, which showed that the recrystallisation temperature range decreased as the particle density increased. Fig. 6 also shows that increasing the original grain-size reduces the recrystallisation rate in each of two alloys representing the extremes of the two-phase composition range; although, as in the isochronal experiments, there is a noticeably greater sensitivity to the effect of original grain-size in the alloy having the lower iron content.

The results of the nucleation counts, as a function of the progress of recrystallisation (fig. 7), show that, for a constant fraction of material recrystallised, a greater density of nuclei exists for the 0.86 wt % iron alloy than for the 0.06 or 0.008 wt % iron alloys. Fig. 7 also shows that, for alloys of constant composition, decreasing the original grain-size increases the nucleation frequency, there again being a greater variation in the case of the alloy having the lower iron content.

Finally, fig. 8 suggests that the variation of nucleation rate implied by fig. 7 is of much greater significance than any variation of the growth rate in controlling the overall recrystallisation kinetics. It is therefore clear that (for the dispersion conditions listed in table I): firstly, the recrystallisation process is accelerated (both isochronally and isothermally) by an increase in the number of dispersed particles and/or by a decrease in the original grain-size; and, secondly, in each case this acceleration is associated with an increase in nucleation frequency.

4.2.4. The Mechanism of Recrystallisation

Other work [34, 35] on the deformation of dispersion alloys has shown that dislocation/particle interactions occur during cold-work, and that, for coarse dispersions, these interactions aid the formation of a cell (sub-grain) structure of the type which is frequently associated with the development of a recrystallisation nucleus. It is therefore suggested that, in the present case, Al_3Fe particles (or more correctly their interfaces with the surrounding solid-solution) act as sites for the formation of recrystallisation nuclei, so that increasing the number of particles present leads to a direct increase in the number of nuclei.

However, the development of these nuclei into new, growing grains will occur within the adjacent solid-solution, the solute content of which has been standardised for all alloys and the deformation structure of which will be uniform. Hence the rate of growth of the new grains should not be significantly influenced by increased particle concentrations, since the high-angle boundaries of such grains will be migrating in a similar solid-solution matrix, regardless of its particle content. Growth of the new grains will therefore continue, at similar rates for each alloy, until impingement with other grains occurs, at which stage the recrystallisation process will be complete. The distance which a migrating boundary travels before impingement will be reduced as the number of nuclei (and, therefore, of migrating boundaries) increases. Hence, as was found in the present work, recrystallisation will be completed more rapidly, with a finer recrystallised grain-size under both isothermal and isochronal conditions, as the particle content increases, the controlling factor being nucleation rather than growth.

The inter-particle spacings of these alloys (see table I) are such that localised deformation at particle/matrix interfaces is unlikely to vary significantly the overall internal energy of the bulk material.* Consequently, the overall stored energy of the cold-worked material, which acts as the driving force for the initiation of recrystallisation, is not believed to be a function of the particle content. Hence, the temperature at

*This was confirmed by a close examination (not reported here) of the cold-worked and recrystallised hardness values of the various alloys. This showed no significant difference in the amount of work-hardening as the particle content was increased, for specimens of similar grain-size; although there was a small increase in the amount of work-hardening with increasing grain-size at constant composition. As in the case of recrystallisation, the magnitude of this effect decreased as the particle content increased.

which isochronal recrystallisation starts does not vary with particle content (for alloys of constant grain-size), despite the increased nucleation rate which results from increases in particle density.

The effect of variations in original grain-size, on the recrystallisation of dispersion alloys, can be postulated in terms of the above model as follows.

The recrystallisation behaviour of alloys having a low particle density will be very similar to that of solid solutions. Increasing the original grain-size will, therefore, raise the temperature at which isochronal recrystallisation commences and decrease the number of active nucleation sites (see section 1). Moreover, the nuclei will not be homogeneously distributed throughout the material, since they will be situated at the original grain-boundaries. Hence, there will be a wide variation in the size and shape of the final recrystallised grains.

However, for a uniformly dispersed alloy, as the particle content increases, nucleation will occur increasingly at particle/matrix interfaces; many of which will be situated in the interiors of the original grains rather than at their boundaries. This will have three effects on the alloy's recrystallisation characteristics.

(*a*) The recrystallisation-start temperature will be less sensitive to grain-size variation, since localised deformation at particles makes less contribution to the overall degree of work-hardening than does that resulting from a change in grain size.*

(*b*) The overall rate of nucleation will be increased, but, since much of this nucleation occurs at particle/matrix interfaces, the variation of nucleus density with grain size will be less pronounced.

(*c*) The nucleation sites will be more homogeneously distributed throughout the bulk of the material. Hence the ultimate recrystallised grain-size will be finer and more uniform.

Each of the above effects has been observed in the present work. Hence, the basic model proposed above, in which inhomogeneous deformation at particle/matrix interfaces and/or at matrix grain boundaries facilitates the formation or recrystallisation nuclei, is consistent with all the observations of the present work.

4.2.5. Comparison with Previous Work

Previous work on two-phase dispersion alloys has shown that in some cases recrystallisation has been accelerated, whereas in others retardation has occurred. In general, these two possibilities appear to be independent of the alloy constituents.† Acceleration has generally been associated with wide inter-particle spacings (e.g. 8 μm for internally oxidised copper [15]). Moreover, Antonione *et al* [36] have recently shown that the nucleation characteristics of accelerated recrystallisation, in iron-based dispersion alloys, were of a similar form to those of the present work (fig. 7) as a function of particle content; whilst English and Backofen [37] have observed new grains forming at the interfaces between widely spaced inclusions and the surrounding solid-solution in an iron-silicon alloy. On the other hand, all reported cases of particle-retarded recrystallisation have occurred in alloys for which the inter-particle spacing has been of the order of 1 μm or less.

These results can be rationalised, in terms of the model proposed above, on the basis of the nucleation mechanism proposed by Hu [38] and discussed by Li [39] (that nuclei are formed by the coalescence of a small number of neighbouring dislocation cells, or sub-grains, which were themselves formed during deformation, with the consequent formation of a mobile high-angle boundary) as follows.

(*a*) *Nucleation* In a homogeneous solid-solution alloy, new grains will be formed predominantly in the vicinity of the original grain-boundaries; and the overall recrystallisation kinetics will be controlled by the grain size, internal energy, and composition of the alloy, and by the annealing temperature, etc. The introduction of a small number of uniformly dispersed, hard particles (whether metallic or non-metallic), to an otherwise unaltered solid-solution, will provide additional nucleation sites at the particle/matrix interfaces, with a consequent acceleration of recrystallisation (as described in section 4.2.4). Further increases in particle density will then lead to a continued and proportionate increase in the nucleation rate.

This trend will continue provided the inter-particle spacing is such that nucleation can occur, both simultaneously and independently,

*See footnote on page 248.

†Acceleration has been observed for dispersions of various oxides in copper [15] and iron [36] matrices, and for intermetallic compounds in iron [37] and aluminium [19, 28]; retardation has been observed for oxide particles in copper [23], aluminium [24], and silver [25], and for intermetallics in copper [18], nickel [26], and aluminium [27-29]. This list is by no means complete.

at all particle/matrix interfaces. However, as the particle density is increased, the inter-particle spacing will be reduced to a critical value (say C_1), at which a nucleus attached to one particle would be viable in itself, if left to form by itself, but not if nuclei start to form simultaneously at several neighbouring particles: since then their embryos will interfere with each other before reaching a viable size. Hence, for particle densities greater than that represented by this critical value, there will be a reduction in the overall nucleation rate, as the inter-particle spacing decreases, since viable nuclei will no longer be produced independently at each particle. Further increases in particle density will then lead to a second critical condition when the inter-particle spacing is of the same order as the diameter of the cell structure in the deformed matrix (say C_2). At this stage, the cell walls are likely to be pinned by the particles, and their coalescence to form viable nuclei will be entirely prevented. Continued decreases in the inter-particle spacing are then likely to cause the basic nucleation mechanism to change to that of strain-induced grain-boundary migration, as described by Beck and Sperry [40] and by Bailey [8], since this is dependent only on events at the original grain-boundaries and not on the coalescence of cells within the matrix sub-structure. In this latter stage, the number of nucleation sites will be very much reduced, being associated only with a small number of the matrix grain boundaries and not with the particles which are situated in the grain interiors.

(*b*) *Growth* In all cases growth will occur by the migration of high-angle boundaries, away from the nucleation sites, through the surrounding matrix. For alloys having inter-particle spacings which are greater than the first postulated critical value (C_1), viable nuclei will be formed at each particle. The migrating boundaries will, in general, therefore, impinge on each other before coming into contact with other particles. Hence, the growth rate will not be significantly different from that of a particle-free solid-solution. However, at spacings which are less than C_1, mobile boundaries, originating at fewer and more widely spaced nucleation sites, will have to move past those particles which have not produced an active nucleus before impinging on other migrating boundaries; in this case, their mobility will be reduced, as compared with a particle-free solid-solution, with a consequent reduction in the recrystallisation growth rate. This effect will occur in two stages: since, for spacings in the range C_2 to C_1, nucleation will have occurred at some but not all of the particles; whereas, for spacings less than C_2, nucleation will only have occurred at the original boundaries, and the new migrating boundaries will have to move past a large number of particles before impinging on each other.

(*c*) *Final grain-size* The above effects can also be expected to influence the final recrystallised grain-size, since there will be a direct relationship between the number of viable nuclei and the number of recrystallised grains which they produce. Hence, particle-accelerated recrystallisation should be typified by a uniformly distributed, fine grain-structure, the grain size of which decreases as the particle density increases; whereas particle-retarded recrystallisation should be typified by a less uniformly distributed, coarse grain-structure resulting from the slow growth of a small number of nuclei.

The present work was confined to alloys with inter-particle spacing not less than 4 μm. Doherty and Martin's results [28] are, therefore, of particular interest, since they concern aluminium-copper alloys with a maximum inter-particle spacing of 4 μm, the particle sizes and isothermal annealing conditions being similar to those used here. Their nucleation and growth rate data are plotted as a function of inter-particle spacing in fig. 11, together with those from the present investigation. This clearly indicates the existence of the two, critical, inter-particle spacing values postulated above. Unfortunately, neither investigation included a direct observation of the dislocation sub-structures involved. However, it is of interest to note that the diameter of the cell structure in heavily deformed aluminium is usually of the order of 1 to 2 μm: since it is expected that the independent formation of viable nuclei at each particle should begin to break down at a spacing which represents approximately two cell diameters (i.e. $C_1 =$ 4 μm, in fig. 11), and should be completely prevented at spacings equal to, or less than, the cell diameter (i.e. $C_2 = 1.8$ μm, in fig. 11).

Furthermore, Doherty and Martin reported that the recrystallisation of an alloy having an inter-particle spacing of 1.2 μm occurred by the strain-induced migration of original grain-boundaries and not by the formation of nuclei

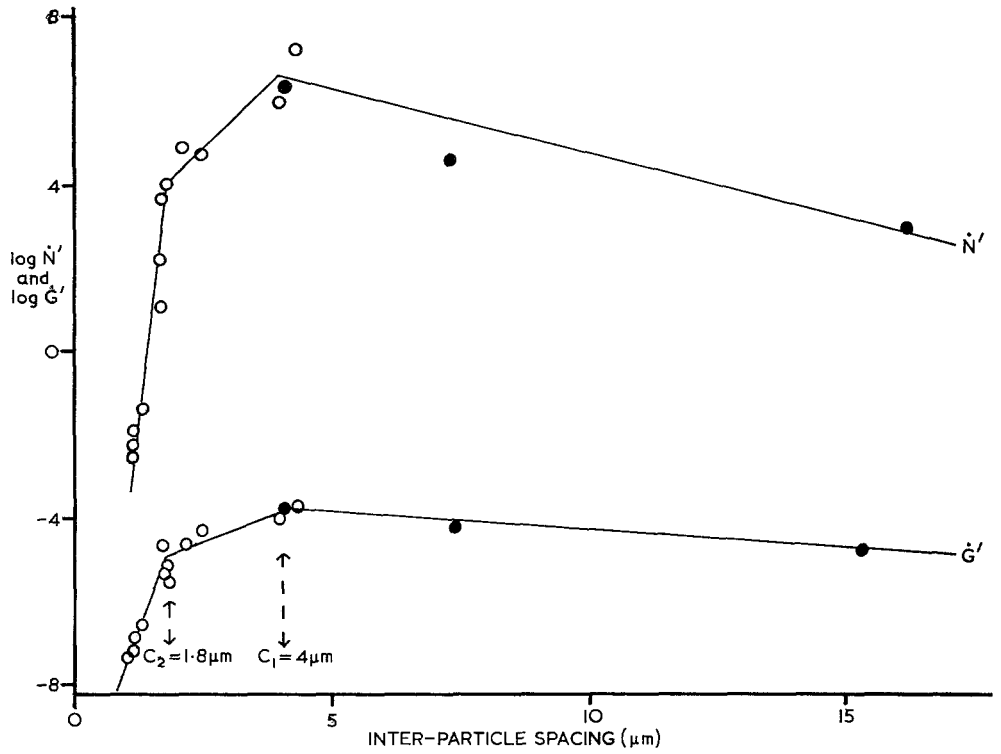

Figure 11 Apparent nucleation and growth rates versus inter-particle spacing for aluminium-copper alloys (O; after Doherty and Martin) and for aluminium-iron alloys (●; present work).

TABLE III Isothermal recrystallisation data for aluminium-copper dispersion alloys annealed at 305° C (after Doherty and Martin [28]).

r (μm)	$2R$ (μm)	$t_{50\%}$ (sec)	$\dot{N}'$	$\dot{G}'$	d_o (mm)	d_r (mm)
Matrix solid solution		1.6×10^3	10^2	10^{-5}	0.56	0.20
0.75	4.0	1.6×10	10^6	10^{-4}	0.52	0.03
0.43	2.5	1.0×10^2	10^4	10^{-4}	0.58	0.06
0.32	1.7	3.8×10^2	10^2	10^{-5}	0.50	0.06
0.24	1.4	1.5×10^4	10^{-1}	10^{-6}	0.52	0.52
0.23	1.2	3.9×10^5	10^{-2}	10^{-7}	0.50	0.59

d_o = average grain-diameter prior to recrystallisation
d_r = average grain-diameter after recrystallisation

at particle/matrix interfaces. Table III also shows that, although the original grain-sizes were similar, the final grain-size for the alloy having an inter-particle spacing of 4 μm was very much finer than that for alloys in which retardation occurred. In particular, for spacings less than 1.7 μm, each original grain produced only one new grain, or less; whereas several nucleation sites must have been present in each original grain at wider inter-particle spacings.

Each of these results, together with the particle-dependent acceleration of nucleation observed by English and Backofen [37] and by Antonione *et al* [36] for wider inter-particle spacings, is consistent with the changes of nucleation and growth mechanisms, as a function of particle content, which form the basis of the present hypothesis.

5. Conclusions

The recrystallisation behaviour of aluminium-iron alloys has been shown to be a function of the iron content and the original grain-size.

(*a*) For solid-solution alloys the temperature at which recrystallisation starts, and the temperature range required to complete the process, both increase as the iron content increases.

(*b*) For two-phase alloys, having inter-particle spacings greater than 4 μm, recrystallisation is accelerated, both isochronally and isothermally, as the number of Al_3Fe particles increases and/or the original matrix grain-size decreases. The influence of grain size becomes less pronounced as the particle content increases. These observations are associated with increases in nucleation rate, owing to nucleation at particle/matrix interfaces and/or at original grain-boundaries, with no significant variation of growth rate.

A hypothesis can be developed comparing the present results with those showing retarded recrystallisation for closer inter-particle spacings, on the assumption that nucleation at particle/matrix interfaces becomes difficult when the inter-particle spacing becomes of the order of twice the diameter of the sub-grain structure of the cold-worked matrix.

Appendices

A.1. Interpretation of Isochronal Recrystallisation Data

For each of the alloys investigated, there was an initial, gradual decrease of hardness with annealing temperature, of the order of 25% of the total softening, which was not accompanied by any visible metallographic change, and which was, therefore, attributed to recovery. The more rapid decrease in hardness occurring at higher temperatures (see fig. 1) coincided with metallographic observations of recrystallisation. The processes of recovery and recrystallisation overlapped to such an extent that it was not possible to ascertain, from the hardness data, the temperature at which recrystallisation started.

Furthermore, the extent of the recovery softening was such, that the temperature at which 50% total softening occurred was significantly different from that corresponding to 50% recrystallisation. The true 50% recrystallisation temperature was therefore calculated, from the hardness data, by measuring the rate of change of hardness with temperature and plotting this against the annealing temperature, giving curves of the type shown in fig. 12, which correspond to the curves of hardness versus temperature (fig. 1). The temperature at which the rate of change of hardness is a maximum was then found to coincide, within experimental error, with the temperature corresponding to 50% recrystallisation, as observed metallographically. This is shown, for the full range of dispersion alloys, in fig. 13, which also shows that the temperature of 50% total softening is consistently lower (by approximately 10° C) than the true 50% recrystallisation temperature. This latter observation implies that the extent of softening due to recovery does not vary as a function of particle content, since any variation of recovery softening would be reflected in a variation of the 50% total softening temperature relative to the true 50% recrystallisation temperature.

Finally, it was also found that the temperature at which the rate of change of hardness decreased to zero, after recrystallisations, coincided with the temperature corresponding to the metallographic observation of the completion of recrystallisation. This is shown in fig. 2.

A.2. The Influence of Particle Size on Isochronal Recrystallisation

Attempts to coarsen the particle size of both as-cast, and cast and forged, two-phase alloys, by single isothermal treatments of up to 112 h at 620° C, were entirely unsuccessful. Experiments were then carried out to measure the electrical resistance of a standard specimen at 24° C, as a function of annealing time, first at 620° C, and then at 450° C, for alloys containing 0.24 and 1.08 wt % iron, respectively. These showed that samples of each alloy, which had previously been in equilibrium at 620° C, attained equilibrium at 450° C in a time of approximately 13 h, and that the time required to re-attain equilibrium at 620° C was then approximately 4 h. As-cast samples of these alloys were then subjected to several series of thermal cycling treatments; each cycle consisting of 5 h at 620° C followed by 19 h at 450° C (i.e. slightly longer than was required to attain constitutional equilibrium at each temperature). Each series of cycles was then completed by a further 5 h treatment at 620° C, in order to avoid the presence of any very fine particles which might have been precipitated at 450° C. The samples were then finally hot-forged. Metallographic examination showed, in each case, that these treatments produced a uniformly distributed dispersion of Al_3Fe particles, the size

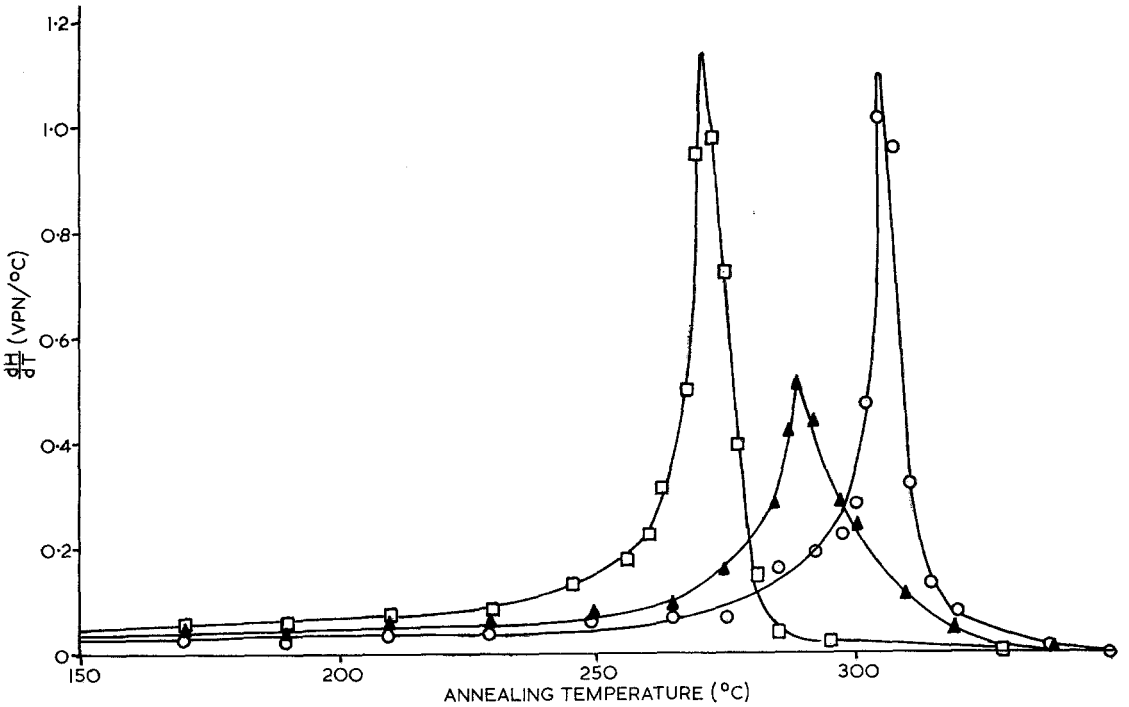

Figure 12 Rate of change of hardness versus annealing temperature for three two-phase alloys, the isochronal annealing curves of which are shown in fig. 1 (□ = 0.4 wt% Fe; ▲ = 0.04 wt % Fe; O = 0.008 wt % Fe).

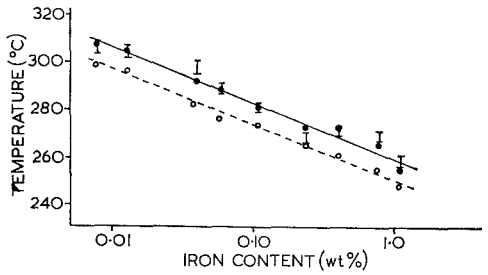

Figure 13 The variation of the 50% recrystallisation temperature and the 50% softening temperature as a function of iron content for two-phase alloys (I = metallography; ● = dH/dT_{max}; O = 50% decrease in hardness).

of which increased, at an exponentially decreasing rate, as the number of cycles increased, although there was no appreciable change of matrix grain size. These results are summarised in table IV.

Further samples of alloys containing 0.01, 0.24, and 1.08 wt % iron were then subjected to a similar series of thermal cycling treatments, prior to preparation for final recrystallisation by the forging and solid-solution standardisation treatments described in section 2.1. The resultant isochronal annealing curves are shown in fig. 14, from which it can be seen that the recrystallisation characteristics of each alloy were completely independent of the thermal cycling treatment. It can, therefore, be concluded that the results reported in the present paper are uninfluenced by the small variation of particle size resulting from the variation of their iron content. (Compare tables I and IV.)

TABLE IV Particle-size and matrix grain-size data as a function of thermal cycling treatment.

Composition	0 cycles		3 cycles		9 cycles		21 cycles	
(wt % iron)	r (μm)	d_0 (mm)	r (μm)	d_0 (mm)	r (μm)	d_0 (mm)	r (μm)	d_0 (mm)
0.24	0.37	0.17	0.60	0.16	0.71	0.17	0.91	0.19
0.08	0.45	0.16	0.73	0.15	0.92	0.14	1.11	0.14

r = average particle-radius
d_0 = average grain-diameter

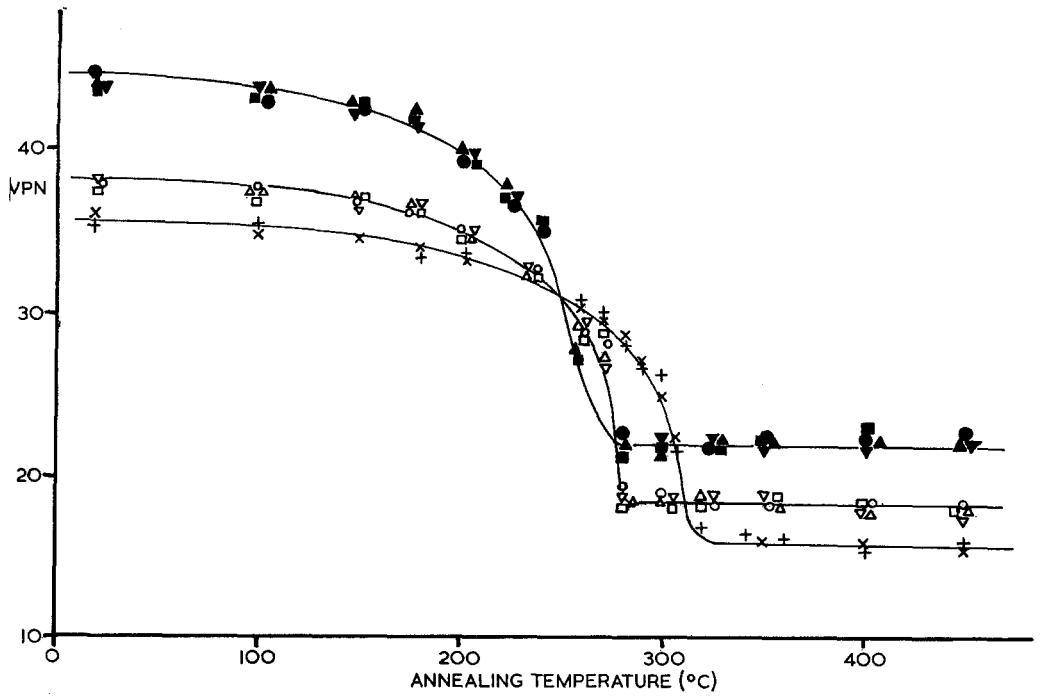

Figure 14 Hardness versus annealing temperature for the three two-phase alloys which had been subjected to thermal cycling treatments (1.08 wt % Fe: ●, 0 cycles; ▼, 3 cycles; ▲, 9 cycles; ■, 21 cycles. 0.24 wt % Fe: O, 0 cycles; ▽, 3 cycles; △, 9 cycles; □, 21 cycles. 0.01 wt % Fe: ×, 0 cycles; +, 21 cycles).

Acknowledgements

The authors are grateful to Professor L. W. Derry for his encouragement and for the provision of laboratory facilities, to Miss M. K. B. Day and Mr S. Walton, of the British Aluminium Co, for the supply of materials and for the helpful discussion, to the British Non-ferrous Metals Research Association for assistance with chemical analysis, and to Professors R. W. Cahn and F. C. Thompson and Drs J. W. Martin and R. D. Doherty for helpful discussions. One of them (P.R.M.) also wishes to thank the Science Research Council for the provision of a maintenance grant throughout the duration of this work.

References

1. L. M. CLAREBROUGH, M. E. HARGREAVES, D. MICHELL, and G. W. WEST, *Proc. Roy. Soc. A* **215** (1952) 507.
2. M. BEVER and L. B. TICKNER, *Acta Met.* **1** (1953) 116.
3. M. E. HARGREAVES, M. H. LORETTO, L. M. CLAREBROUGH, and R. L. SEGALL, "Recovery and Recrystallisation of Metals", edited by L. Himmel (Interscience, 1963), p. 63.
4. M. H. LORETTO and A. J. WHITE, *Acta Met.* **9** (1961) 512.
5. H. CONRAD and B. CHRIST (op. cit. ref. 3), p. 124.
6. O. JOHARI and G. THOMAS, *Acta Met.* **12** (1964) 679.
7. P. A. BECK and P. R. SPERRY, *J. Appl. Phys.* **21** (1950) 150.
8. J. E. BAILEY, *Phil. Mag.* **5** (1960) 833.
9. J. E. BAILEY and P. B. HIRSCH, *Proc. Roy Soc. A* **267** (1962) 11.
10. P. W. DAVIES, A. P. GREENOUGH, and B. WILSHIRE, *Phil. Mag.* **6** (1961) 795.
11. M. COOK and T. LL. RICHARDS, *J. Inst. Met.* **73** (1947) 1.
12. T. K. AUST and J. W. RUTTER, *Trans. Met. Soc. Amer. Inst. Min. Metall. Engrs.* **218** (1960) 682.
13. K. LÜCKE and K. DETERT, *Acta Met.* **5** (1957) 628.
14. K. LÜCKE and P. STÜWE (op. cit. ref. 3), p. 171.
15. J. W. MARTIN, *Metallurgia* **55** (1957) 161.
16. T. LL. RICHARDS and S. F. PUGH, *J. Inst. Met.* **88** (1959) 141.
17. W. M. WILLIAMS and R. EBORALL, *ibid* **81** (1952) 501.
18. V. A. PHILLIPS and A. PHILLIPS, *ibid*, p. 185.
19. M. K. B. DAY, *Mem. Sci. Rev. Mét.* **56** (1959) 201.
20. R. L. RICKETT and C. W. LESLIE, *Trans. Amer. Soc. Metals* **51** (1959) 310.

21. P. A. BECK, *Trans. Amer. Inst. Min. Metall. Engrs.* **137** (1940) 234.
22. E. A. BLOCH, *Met. Rev.* **6** (1961) 193.
23. M. ADACHI and N. J. GRANT, *Trans. Met. Soc. Amer. Inst. Min. Metall. Engrs.* **218** (1960) 881.
24. O. PRESTON and N. J. GRANT, *ibid* **221** (1961) 164.
25. A. GATTI and R. FULLMAN, *ibid* **215** (1959) 762.
26. K. DETERT and J. ZIEBS, *ibid* **233** (1965) 51.
27. N. RYUM, *J. Inst. Met.* **94** (1966) 191.
28. R. D. DOHERTY and J. W. MARTIN, *ibid* **91** (1962) 332.
29. *Idem, Trans. Amer. Soc. Metals* **57** (1964) 874.
30. A. SAULNIER, M. CROUTZEILLES, and P. MIRAND, "Proceedings of the Fifth International Conference on Electron Microscopy" (Academic Press, 1962), p. K2.
31. R. B. SHAW, L. A. SHEPARD, L. A. STARR, and J. E. DORN, *Trans. Amer. Soc. Metals* **45** (1953) 249.
32. J. E. HILLIARD and R. W. CAHN, *Trans. Met. Soc. Amer. Inst. Min. Metall. Engrs.* **221** (1961) 344.
33. J. K. EDGAR, *ibid* **180** (1949) 225.
34. P. R. SWANN, Symposium on "Electron Microscopy and Strength of Solids" (Interscience, 1963).
35. W. C. LESLIE, J. T. MICHALAK, and F. W. AUL, "Iron and Its Dilute Solid-Solutions" (AIME, 1963), p. 119.
36. C. ANTONIONE, G. DELLA GATTA, and G. VENTURELLO, *Trans. Met. Soc. Amer. Inst. Min. Metall. Engrs.* **230** (1964) 700.
37. A. T. ENGLISH and W. A. BACKOFEN, *ibid*, p. 396.
38. H. HU (op. cit. ref. 3), p. 311.
39. J. M. C. LI, *J. Appl. Phys.* **33** (1962) 2958.
40. P. A. BECK and P. R. SPERRY, *ibid* **21** (1950) 150.